mathematics

Article

Numerical Reconstruction of Time-Dependent Boundary Conditions to 2D Heat Equation on Disjoint Rectangles at Integral Observations

Miglena N. Koleva [1,*] and Lubin G. Vulkov [2]

1 Department of Mathematics, Faculty of Natural Sciences and Education, University of Ruse, 8 Studentska Str., 7017 Ruse, Bulgaria
2 Department of Applied Mathematics and Statistics, Faculty of Natural Sciences and Education, University of Ruse, 8 Studentska Str., 7017 Ruse, Bulgaria; lvalkov@uni-ruse.bg
* Correspondence: mkoleva@uni-ruse.bg; Tel.: +359-82-888-587

Abstract: In this paper, two-dimensional (2D) heat equations on disjoint rectangles are considered. The solutions are connected by interface Robin's-type internal conditions. The problem has external Dirichlet boundary conditions that, in the forward (direct) formulation, are given functions. In the inverse problem formulation, the Dirichlet conditions are unknown functions, and the aim is to be reconstructed upon integral observations. Well-posedness both for direct and inverse problems is established. Using the given 2D integrals of the unknown solution on each of the domains and the specific interface boundary conditions, we reduce the 2D inverse problem to a forward heat 1D one. The resulting 1D problem is solved using the explicit Saul'yev finite difference method. Numerical test examples are discussed to illustrate the efficiency of the approach.

Keywords: heat equation; disjoint domains; inverse problem; integral observation; difference scheme; Saul'yev method

MSC: 65M06; 65M32

check for updates

Citation: Koleva, M.N.; Vulkov, L.G. Numerical Reconstruction of Time-Dependent Boundary Conditions to 2D Heat Equation on Disjoint Rectangles at Integral Observations. *Mathematics* **2024**, *12*, 1499. https://doi.org/10.3390/math12101499

Academic Editors: Fajie Wang and Ji Lin

Received: 17 April 2024
Revised: 4 May 2024
Accepted: 8 May 2024
Published: 11 May 2024

1. Introduction

Inverse problems arise in the modeling of many physical and social processes [1,2]. Most of these models are dynamical; thus, they are governed by evolution differential equations. If all essential parameters, including coefficients, sources, and initial and boundary conditions in the evolutionary equation problem, are provided, the solution can be calculated, enabling the prediction of the process's behavior under different conditions. However, in processes involving, for example, chemical diffusion, heat conduction, and population dynamics (such as honey bee populations), certain inputs such as the coefficients and boundary conditions of the differential equations are unknown and need to be reconstructed based on additional state observations. Such problems are usually ill-posed [2–7], and they are difficult to solve, even numerically.

One class of such identification problems is inverse problems, where the boundary condition(s) have to be determined. Recently, many papers concerning boundary inverse problems for diffusion equations of integer and fractional orders have been published.

The authors of [8] solved the inverse problem of recovering an unknown boundary condition in a parabolic problem from given observations at a boundary point. In [9], by applying a semigroup approach, the authors study boundary inverse problems for a linear parabolic equation. A numerical method, based on the decomposition technique, for solving the inverse problem of recovering the unknown boundary condition of a heat conduction equation is proposed in [10].

The inverse problem for boundary condition determination in time-fractional diffusion and equations on the basis of overspecified data is studied, for example, in [11–14]. The existence and uniqueness of the inverse problem is established in [11,13]. The authors of [13] apply a meshless method based on radial basis functions to solve the inverse problem. In [12,14], a spectral regularization technique is introduced, which relies on the solution provided by the Fourier method, to address the Cauchy problem for time-fractional diffusion and advection–dispersion equations.

The heat equation has many real-life applications; see, e.g., [15,16]. Various phenomena in fields such as ecology, biology, heat and mass transfer, and material science encompass diffusion processes across materials. For instance, [17] presents a model of diffusion-limited contamination and decontamination in a two-layer porous medium. Additionally, multilayer diffusion in a composite medium with imperfect contact is investigated in [18]. In [19], the authors examine how coupled heat and mass transfer affect the peristaltic motion of a magnetohydrodynamic stress–strain Jeffery-type hybrid nanofluid flowing through an inclined asymmetric micro-channel with a porous medium. The fractionalized flow and thermal transmission of a Brinkman-type tri-hybrid nanofluid over an infinite plate saturated in a porous medium are studied in [20]. Semi-analytical and numerical solutions for transport in a multi-layered profile are constructed, for example, in [21–24].

The basic model motivating the present paper is that of heat conduction in multiple species on different layers, where the effect of the intermediate region (layer) is modeled by special nonlocal jump conditions across the layer [24–29].

In [30], the authors consider one transient heat conduction problem in 1D multilayered slabs, cylinders, and spheres. They propose an analytical solution, based on the computation of the eigenvalues and the eigenfunctions of the resulting Sturm–Liouville-type system. The Fokas transform method is implemented in [31] to solve a multidomain linear reaction–diffusion equation with a discontinuous diffusion coefficient in order to investigate highly diffusive brain tumors while also considering the heterogeneity of brain tissue.

A second order in space finite volume scheme for solving multilayer diffusion problems is developed in [24]. In [27,29], the authors obtain an a priori estimate in Sobolev-like space for the weak solution of 1D and 2D parabolic problems on a disconnected domain. To solve the problem, a finite difference scheme is constructed and analyzed. In [26], a strong solution using the finite difference method for a parabolic problem on a disjoint domain is investigated.

One-dimensional boundary identification and backward heat conduction problems for layer materials are studied in [32]. In our previous works, we constructed a decomposition method to recover external boundary conditions in a time-fractional parabolic problem [33] and a hyperbolic–parabolic problem [34] on disjoint domains under point measurements.

Saul'yev asymmetric methods [35] have been used to solve a large class of integer and fractional order partial differential equations; see, e.g., [36–40]. In general, these schemes are unconditionally stable and first-order accurate, and they have an implicit form but can be realized explicitly. The restriction of the ratio between the time and square of the space step size is because of the consistency. The main advantage of this numerical method is computational efficiency.

In this work, we construct an explicit numerical method for solving the inverse problem to identify external Dirichlet boundary conditions in a 2D parabolic problem, defined on disjoint domains with imposed Dirichlet, Neumann, and interface boundary conditions. The approach is based on the idea presented in [41] to formulate the inverse problem as a one-dimensional problem, resolved by the Saul'yev method. We extend this conception for a more complicated problem, where we have to overcome the interface boundary and domain disconnectedness. Our method also differs in the construction of the approximations of the Neumann boundary conditions of the 2D direct problem. Moreover, special attention is paid to discretization at the corner nodes, where the interface boundary intersects with the Neumann boundary. The numerical scheme is constructed in a manner that decouples the problem at each time layer, namely, each solution can be computed in its own domain.

The paper is structured as follows. In the next section, we present the direct (forward) interface problem and establish well-posedness. In Section 3, we formulate the inverse problem, prove the well-posedness and describe the algorithm that reduces the two-dimensional inverse problem into the one-dimensional one. By applying the Saul'yev method [35], we realize the analytical approach through the explicit finite difference method in Section 4. Numerical tests are discussed in Section 5 and then the paper ended with some conclusions.

2. Direct Problem

In this section, we introduce the direct (forward) problem and discuss its well-posedness.

2.1. Formulation of the Problem

First, we formulate the 2D direct problem. As a model example, we consider the following initial boundary value problem, defined on disjoint domains; see Figure 1.

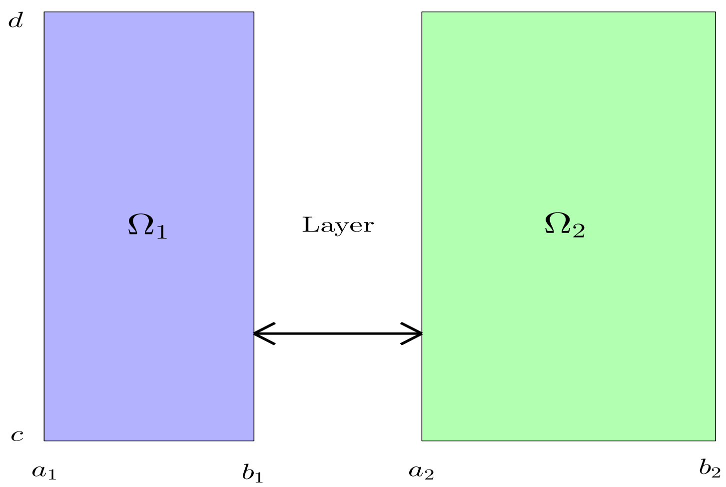

Figure 1. Spatial domain of the problem (1)–(8): two disconnected rectangles Ω_1, Ω_2; the solution is coupled by interface conditions (7), (8) at $x = b_1$ and $x = a_2$.

$$\frac{\partial u_1}{\partial t} = p_1 \frac{\partial^2 u_1}{\partial x^2} + q_1 \frac{\partial^2 u_1}{\partial y^2} + f_1(x,y,t), \quad (x,y,t) \in Q_{1T} = \Omega_1 \times (0,T] \tag{1}$$

$$\frac{\partial u_2}{\partial t} = p_2 \frac{\partial^2 u_2}{\partial x^2} + q_2 \frac{\partial^2 u_2}{\partial y^2} + f_2(x,y,t), \quad (x,y,t) \in Q_{2T} = \Omega_2 \times (0,T] \tag{2}$$

where $\Omega_i = (a_i, b_i) \times (c,d)$, with Dirichlet and Neumann external boundary conditions

$$u_1(a_1,y,t) = \mu_1(y)\varphi_1(t), \quad c \le y \le d, \quad 0 < t \le T \tag{3}$$

$$u_2(b_2,y,t) = \mu_2(y)\varphi_2(t), \quad c \le y \le d, \quad 0 < t \le T \tag{4}$$

$$\frac{\partial u_1}{\partial y}(x,c,t) = g_{1c}(x,t), \quad \frac{\partial u_1}{\partial y}(x,d,t) = g_{1d}(x,t), \quad a_1 \le x \le b_1 \tag{5}$$

$$\frac{\partial u_2}{\partial y}(x,c,t) = g_{2c}(x,t), \quad \frac{\partial u_2}{\partial y}(x,d,t) = g_{2d}(x,t), \quad a_2 \le x \le b_2 \tag{6}$$

and interface mixed-type boundary conditions

$$p_1 \frac{\partial u_1}{\partial x}(b_1,y,t) + \alpha_1 u_1(b_1,y,t) = \beta_1 u_2(a_2,y,t) + \gamma_1(y,t), \quad c \le y \le d, \quad 0 < t \le T \tag{7}$$

$$-p_2 \frac{\partial u_2}{\partial x}(a_2,y,t) + \alpha_2 u_2(a_2,y,t) = \beta_2 u_1(b_1,y,t) + \gamma_2(y,t), \quad c \le y \le d, \quad 0 < t \le T \tag{8}$$

where $-\infty < a_1 < b_1 < a_2 < b_2 < +\infty$ and $-\infty < c < d < +\infty$.

The problem (1)–(8) is completed by the initial conditions

$$u_i(x, y, 0) = u_i^0(x, y), \quad (x, y) \in \overline{\Omega}_i = [a_i, b_i] \times [c, d], \quad i = 1, 2 \tag{9}$$

Further, we assume that

$$\alpha_i > 0, \quad \beta_i > 0, \quad i = 1, 2 \tag{10}$$

In Equations (1) and (2), u_1 and u_2 can represent temperature fields in a two slabs. The interface conditions in Equations (7) and (8) are specific to this problem and describe the heat interaction of the slabs. For example, Equation (7) specifies that the flux $p_1 \frac{\partial u_1}{\partial x}(b_1, y, t)$ is proportional to the proportionality coefficients (contact transfer coefficients) α_1 and β_1, to the difference in the temperatures $u_2(a_2, y, t)$ and $u_1(b_1, y, t)$ of the slabs, and to the heat source $\gamma_1(y, t)$.

A motivated heat–mass transfer process that leads to the one-dimensional version of the present forward problem is described in [42].

The *direct (forward) problem* is to find the solutions $u_1(x, y, t)$ and $u_2(x, y, t)$ of Equations (1) and (2) at the given initial, boundary, and interface conditions (3)–(9).

2.2. Well-Posedness of the Direct Problem

In order to establish the well-posedness of the direct problem, i.e., existence, uniqueness, and continuous dependence from the input data, we follow the results from [27].

Without a loss of generality, we can suppose that the external Dirihlet boundary conditions (3) and (4) are zero, as well as $\gamma_i(y, t) = 0$, $i = 1, 2$. Otherwise, this can be archived by applying linear transformations like those in [33].

We use the product Hilbert space

$$L = L_2(\Omega_1) \times L_2(\Omega_2) = \{w = (w_1, w_2) : w_j \in L_2(\Omega_i),\ j = 1, 2\}$$

subjected to the inner product and the corresponding norm

$$(v, w)_L = (v_1, w_1)_{L_2(\Omega_1)} + (v_2, w_2)_{L_2(\Omega_2)}, \quad \|w\|_L = (w, w)_L^{1/2}$$

with

$$(v_j, w_j)_{L_2(\Omega_j)} = \int_{\Omega_j} v_j w_j dxdy, \quad j = 1, 2$$

Next, we introduce the Sobolev spaces

$$H^l := \{w = (w_1, w_2) : w_j \in H^1(\Omega_j)\}, \quad l = 1, 2, \ldots$$

subjected to the inner products and norms

$$(v, w)_{H^l} = (v_1, w_1)_{H^l(\Omega_1)} + (v_2, w_2)_{H^l(\Omega_2)} \quad \|w\| = (w, w)_{H^l}^{1/2},$$

with

$$(w_j, v_j)_{H^l(\Omega_j)} = \sum_{S=0}^{l} \sum_{m=0}^{S} \left(\frac{\partial^S w_j}{\partial x^m \partial y^{S-1}}, \frac{\partial^S v_j}{\partial x^m \partial y^{S-1}} \right)_{L_2(\Omega_j)}, \quad j = 1, 2, \quad l = 1, 2, \ldots$$

Now, we are able to introduce the bilinear form:

$$\begin{aligned} A(u, w) = {} & \int_{\Omega_1} \left(p_1 \frac{\partial u_1}{\partial x} \frac{\partial w_1}{\partial x} + q_1 \frac{\partial u_1}{\partial y} \frac{\partial w_1}{\partial y} \right) dxdy + \int_{\Omega_2} \left(p_2 \frac{\partial u_2}{\partial x} \frac{\partial w_2}{\partial x} + q_2 \frac{\partial u_2}{\partial y} \frac{\partial w_2}{\partial y} \right) dxdy \\ & + \alpha_1 u_1(b_1, y) w_1(b_1, y) + \alpha_2 u_2(a_2, y) w_2(a_2, y) \\ & - \beta_1 u_2(a_2, y) w_1(b_1, y) - \beta_2 u_1(b_1, y) w_2(a_2, y) \end{aligned}$$

Next, by applying Theorem 26.1 of [43], we prove the boundedness and weak definiteness of the bilinear form A. Now, for the bilinear form $A(u,w) = A(t;u,v)$, the following applies.

Lemma 1. *Suppose that the conditions (10) are fulfilled. Then, the bilinear form $A(u,w) = A(t;u,w)$, measurable on $[0,T]$, is bounded on $H^1 \times H^1$, and A satisfies the Garding inequality on H^1*

$$A(u,u) + k\|u\|_L^2 \geq m\|u\|_H^2, \quad \forall\, u \in H^1$$

where k and m are positive constants.

Further, we need the following facts from the theory of Hilbert spaces; see, e.g., [43].

Let Ω be bounded in R^n and $v(t)$ be a function mapping from Ω to a Hilbert space H. We introduce the Sobolev space of vector-valued functions $H^l(\Omega, H)$, subjected to the inner product

$$(v,w)_{H^l(\Omega,H)} = \int_\Omega \sum_{|\beta|\leq l} (D^\beta v(t), D^\beta w(t))_H dt, \quad l = 0,1,2,m$$

Let $H^{1/2}(0,T)$ be the fractional Sobolev space, as defined in [43,44]. We define the space $L_2(\Omega,H) = H^0(\Omega,H)$, $H^{1,1/2} = L_2((0,T),H^1) \cap H^{1/2}((0,T),L)$ and the space

$$W(0,T) = \{v : v \in L_2(v|v \in L_2((0,T),H^1), \frac{\partial u}{\partial t} \in L_2((0,T),L))\}$$

subjected to the inner product

$$(v,w)_{w(0,T)} = \int_0^T \left[(v(\cdot,t), w(\cdot,t))_{H^1} + \left(\frac{\partial v}{\partial t}(\cdot,t), \frac{\partial w}{\partial t}(\cdot,t) \right)_L \right] dt$$

Now, the weak formulation of the problem (1)–(9) is as follows: for $\forall\, w \in L_2((0,T),H^1)$, find u satisfying the identity

$$\left(\frac{\partial u}{\partial t}(\cdot,t), w(\cdot,t) \right)_L + A(u(\cdot,t), w(\cdot,t)) = (f(\cdot,t), w(\cdot,t))_L$$

Theorem 1. *If (10) holds and $u^0 = (u_1^0, u_2^0) \in L$, $f = (f_1,f_2) \in L_2((0,T),L)$, then the initial boundary value problem (1)–(9) have a unique weak solution $u \in W(0,T)$, and it depends continuously on u^0 and f.*

Proof. We apply the theory of differential operators in Hilbert spaces [43] to the problem (1)–(9). First, let us note that the all of the above, starting with Lemma 1, are preparation for the proof. Namely, we use the theory for parabolic equations in Chapter 4 of [43]. Then, following the methods used in [27], we apply Theorem 26.1 from [43] to obtain the results of the present theorem. □

3. Inverse Problem

This section formulates and studies the inverse problem. First, using the integral observation, we reduce the 2D inverse problem to an equivalent 1D direct one. Then, we prove the well-posedness of the new 1D problem, from which we can obtain the existence and uniqueness of the solution to the original 2D inverse problem.

In the Dirichlet *external boundary conditions* (3) and (4), let the function $\varphi_i(t)$, $i = 1,2$ be *unknown*; they have to be identified using some over-specified data.

The *inverse problem* (IP) for identifying the function $\varphi_i(t)$, $i = 1,2$ in the external boundary conditions (3) and (4) can be formulated as follows:

IP: Find $(u_1(x,y,t), u_2(x,y,t), \varphi_1(t), \varphi_2(t))$, if the following integral observations are imposed:

$$\int_{a_i}^{b_i}\int_c^d u_i(x,y,t)dxdy = m_i(t), \quad i = 1,2, \quad 0 \le t \le T \tag{11}$$

This shows that if $u_i(x,y,t)$, $i = 1,2$ are temperature, the mean temperature of each of the slabs is measured and the results are $m_i(t)$, $t \in [0,t]$, $i = 1,2$.

3.1. Reducing the Two-Dimensional Inverse Problem to One-Dimensional Ones

Here, we propose the main strategy to design a method for the reduction of the 2D inverse problem to a simple 1D direct problem.

We introduce the function

$$v_i(x,t) = \int_c^d u_i(x,y,t)dy, \quad a_i \le x \le b_i, \quad 0 \le t \le T, \quad i = 1,2 \tag{12}$$

Then, from (1) and (2), we obtain the equation

$$\frac{\partial v_i}{\partial t} - p_i\frac{\partial^2 v_i}{\partial x^2} - \widetilde{q}_i(x,t) = \widetilde{f}_i(x,t), \quad a_i \le x \le b_i, \quad 0 \le t \le T, \quad i = 1,2 \tag{13}$$

where

$$\widetilde{q}_i(x,t) = q_i\big(g_{id}(x,t) - g_{ic}(x,t)\big), \quad \widetilde{f}_i(x,t) = \int\limits_c^d f(x,y,t)dy \quad i = 1,2$$

with initial conditions

$$v_i(x,0) = v_i^0(x) = \int_c^d u_i^0(x,y)dy, \quad a_i \le x \le b_i, \quad 0 \le t \le T, \quad i = 1,2 \tag{14}$$

external boundary conditions

$$v_1(a_1,t) = \varphi_1(t)\int_c^d \mu_1(y)dy, \quad 0 \le t \le T \tag{15}$$

$$v_2(b_2,t) = \varphi_2(t)\int_c^d \mu_2(y)dy, \quad 0 \le t \le T \tag{16}$$

and interface mixed-type boundary conditions

$$p_1\frac{\partial v_1}{\partial x}(b_1,t) + \alpha_1 v_1(b_1,t) = \beta_1 v_2(a_2,t) + \widetilde{\gamma}_1(t), \quad \theta \le t \le T \tag{17}$$

$$-p_2\frac{\partial v_2}{\partial x}(a_2,t) + \alpha_2 v_2(a_2,t) = \beta_2 v_1(b_1,t) + \widetilde{\gamma}_2(t), \quad 0 \le t \le T \tag{18}$$

$$\widetilde{\gamma}_i(t) = \int\limits_c^d \gamma_i(y,t)dt, \quad i = 1,2$$

The overspecified data (11) take the form

$$\int_{a_i}^{b_i} v_i(x,t)dx = m_i(t), \quad i = 1,2, \quad 0 \le t \le T \tag{19}$$

Equation (13) is obtained by integrating (1) and (2) over the interval $[c,d]$ and then integration by parts is used for the boundary conditions (5)–(6). The interface and external Dirichlet boundary conditions are obtained in the same manner—by integrating over the interval $[c,d]$ and using (12). Finally, the non-local conditions (19) directly follow from (11).

From (15) and (16), one calculates

$$\varphi_1(t) = \frac{v_1(a_1,t)}{\int\limits_c^d \mu_1(y)dy}, \quad \varphi_2(t) = \frac{v_2(b_2,t)}{\int\limits_c^d \mu_2(y)dy} \tag{20}$$

Therefore, the inverse problem IP is reduced to the determination of the boundary values $v_1(a_1,t)$ and $v_2(b_2,t)$ from the observations (19).

3.2. Well-Posedness of the Inverse Problem

In this subsection, we prove the well-posedness of the direct problem (13)–(19), from which the well-posedness of the inverse problem follows.

Theorem 2. *Assume that $f = (f_1, f_2) \in L_2(0,T;L(\Omega))$, $u^0 = (u_1,u_2) \in L$, $\gamma = (\gamma_1,\gamma_2) \in L_2(c,d)$. Then, the problem (13)–(19) has a unique solution $v = (v_1,v_2) \in H^{1,0} = L_2(0,T;H^1)$, which satisfies the following weak formulation:*

$$\begin{aligned}
-\beta_2 \int\limits_{Q_{1T}} v_1 \frac{\partial \phi_1}{\partial t} dxdt - \beta_1 \int\limits_{Q_{2T}} v_2 \frac{\partial \phi_2}{\partial t} dxdt + \int\limits_0^T A(v(\cdot,t),\phi(\cdot,t))dt \\
= \quad \beta_2 \int\limits_{\Omega_1} v_1^0(x)\phi_1(x,0)dx + \beta_1 \int\limits_{\Omega_2} v_2^0(x)\phi_2(x,0)dx \\
+\beta_2 \int\limits_{\Omega_1} u_1^0(x)\phi_1(x,0)dx + \beta_1 \int\limits_{\Omega_2} u_2^0(x)\phi_2(x,0)dx \\
+\beta_2 \int\limits_{Q_{1T}} (\widetilde{f}_1(x,t) + \widetilde{q}_1(x,t))\phi_1 dxdt + \beta_1 \int\limits_{Q_{2T}} (\widetilde{f}_2(x,t) + \widetilde{q}_2(x,t)\phi_2 dxdt
\end{aligned}$$

where $\phi_i(x,t) \in H^1(Q_{iT})$, $i = 1,2$ and $\phi_i(x,T) = 0$ are a pair of test functions, $\phi = (\phi_1, \phi_2)$, and

$$\begin{aligned}
\widetilde{A}(v(\cdot,t),\phi(\cdot,t))dt \quad = \quad & \sum_{i=1}^{2} \beta_{3-i} p_i \int\limits_{\Omega_i} \frac{\partial v_i}{\partial x}\frac{\partial \phi_i}{\partial x} dx \\
& - \sum_{i=1}^{2} (-1)^{3-i} (\phi_i(b_i,t) - \phi_i(a_i,t))(\beta_1\beta_2 v_{3-i}(a_{3-i},t) - \beta_{3-i}\alpha_i v_i(b_i,t)) \\
& + \sum_{i=1}^{3} p_i \beta_{3-i} (-1)^{3-i} (\phi_i(b_i,t) - \phi_i(a_i,t))\widetilde{\gamma}_i(t)
\end{aligned}$$

Proof. We differentiate both sides of (19) and then use the Equations (12) and (13) to derive

$$p_i \frac{\partial v_i}{\partial x}(b_i,t) - p_1 \frac{\partial v_i}{\partial x}(a_i,t) + \hat{f}_i(t) = \frac{dm_i}{dt}, \quad i = 1,2 \tag{21}$$

where

$$\hat{f}_i(t) = \int\limits_{a_i}^{b_1} (\widetilde{f}_i(x,t) - \widetilde{q}_i(x,t)dx), \quad i = 1,2$$

Further, we have

$$-p_1 \int\limits_{Q_{1T}} \frac{\partial^2 v_1}{\partial x^2}\phi_1(x,t)dxdt$$
$$= \int\limits_0^T \left(p_1 \frac{\partial v_1}{\partial x}(b_1,t)\phi_1(b_1,t) - p_1 \frac{\partial v_1}{\partial x}(a_1,t)\phi_1(a_1,t) - p_1 \int\limits_{Q_{1T}} \frac{\partial v_1}{\partial x}\frac{\partial \phi_1}{\partial x}dxdt \right)$$

The use of (21), $i = 1$, and (17) leads to

$$\int\limits_{Q_{1T}} p_1 \frac{\partial^2 v_1}{\partial x^2}\phi_1(x,t)dxdt = \int_0^T \left[\left(\phi_1(b_1,t) - \phi_1(a_1,t)\right)\left(\beta_1 v_2(a_2,t) - \alpha_1 v_1(b_1,t)\right)\right]dt$$
$$+ \int_0^T \left[\left(\phi_1(b_1,t) - \phi_1(a_1,t)\right)\widetilde{\gamma}_1(t) + \left(\frac{dm_1}{dt} - \bar{f}_1(t)\right)\phi_1(a_1,t)\right]dt - \int\limits_{Q_{1T}} p_1 \frac{\partial v_1}{\partial x}\frac{\partial \phi_1}{\partial x}$$

In a similar way, using (21), $i = 2$, and (18), we obtain

$$\int\limits_{Q_{2T}} p_2 \frac{\partial^2 v_2}{\partial x^2}\phi_2(x,t)dxdt = \int_0^T \left[\left(\phi_2(b_2,t) - \phi_2(a_2,t)\right)\left(\alpha_2 v_2(a_2,t) - \beta_2 v_1(b_1,t)\right)\right]dt$$
$$+ \int_0^T \left[-\left(\phi_2(b_2,t) - \phi_2(a_2,t)\right)\widetilde{\gamma}_2(t) + \left(\frac{dm_2}{dt} - \bar{f}_2(t)\right)\phi_2(b_2,t)\right]dt - \int\limits_{Q_{2T}} p_2 \frac{\partial v_2}{\partial x}\frac{\partial \phi_2}{\partial x}$$

Further, using the inequality from [44]

$$g^2(t) \le \frac{2}{\varepsilon}\|g\|^2_{L_2(0,T)} + 2\varepsilon\left\|\frac{dg}{dt}\right\|_{L_2(0,T)}, \ \ \varepsilon \in (0,T), \ \ g \in H^1(0,T)$$

together with the Poincare-type inequality

$$\int_{\Omega_i} w_i^2(x)dx \le \frac{b_i^2 - a_i^2}{2}\int_{\Omega_i}\left(\frac{dw_i}{dx}(x)\right)^2 dx, \ \ i = 1,2$$

we prove that for $A\big(v(\cdot,t),\phi(\cdot,t)\big)$, Lemma 1 holds.

This completes the proof of the theorem. □

As a consequence of Theorem 2 and (20), we deduce that the functions $\varphi_i(t)$, $i = 1,2$ are uniquely determined.

4. Numerical Solution of the Direct and Inverse Problems

We follow the strategy proposed in [41] to use the Saul'yev scheme in order to recover $\varphi_i(t)$, $i = 1,2$ numerically; but, in our case, we apply both first- and second-kind approximations and pay special attention to the discretization of the interface conditions. Then, the 2D direct problem (1)–(9) is discretized by the right and left Saul'yev schemes, which can be implemented explicitly. To this aim, we construct a suitable approximation for the Neumann boundary conditions, different from that in [41]. Moreover, interface conditions and conditions on the corner nodes, where the interface boundary intersects with the Neumann boundary, are also overcome. At each time layer, the computations in the first domain are performed from the upper right corner to the lower left corner (a backward method), while in the second domain, we start from the bottom left corner and move to the upper right corner (a forward method). This is possible because the numerical scheme is constructed such that at each time layer, the solution u_1^{n+1} does not depends on u_2^{n+1}, and conversely, the solution u_2^{n+1} does not depend on u_1^{n+1}.

Note that using forward and backward methods in one and the same domain and then averaging the result leads to an improvement in the order of accuracy [45]. Here, we use these methods in different domains, and the idea is to move from a known boundary to an unknown boundary in order to solve the inverse problem.

Let us introduce uniform temporal and spatial meshes:

$$\begin{aligned}
\overline{\omega}_{h_i} &= \{x_{ij_i} = a_i + j_i h_i,\ \ j_i = 0,1,\dots,N_i,\ \ h_i = (b_i - a_i)/N_i\},\ \ i = 1,2 \\
\overline{\omega}_{h_y} &= \{y_s = c + s h_y,\ \ s = 0,1,\dots,N_y,\ \ h_y = (d-c)/N_y\} \\
\overline{\omega}_{\tau} &= \{t_n = n\tau,\ \ n = 0,1,\dots,M,\ \ \tau = T/M\}
\end{aligned}$$

The values of the mesh function w_i in the 1D case at grid node (x_{ij_i}, t_n) are denoted by $(w_i)^n_{j_i}$, and, similarly, the values of the mesh function w_i in the 2D case at grid node (x_{ij_i}, y_s, t_n) are denoted by $(w_i)^n_{j_i,s}$.

4.1. Numerical Solution of the Inverse Problem

Following the Saul'yev idea [35], we approximate (13) for $i = 1$ using the second kind formula and (13) for $i = 2$ using the first kind formula to derive

$$\frac{(v_1)^{n+1}_{j_1} - (v_1)^n_{j_1}}{\tau} - p_1 \frac{(v_1)^{n+1}_{j_1+1} - (v_1)^{n+1}_{j_1} - (v_1)^n_{j_1} + (v_1)^n_{j_1-1}}{h_1^2} = (\widetilde{q}_1)^{n+1}_{j_1} + (\widetilde{f}_1)^{n+1}_{j_1} \tag{22}$$

$$\frac{(v_2)^{n+1}_{j_2} - (v_2)^n_{j_2}}{\tau} - p_2 \frac{(v_2)^{n}_{j_2+1} - (v_2)^{n}_{j_2} - (v_2)^{n+1}_{j_2} + (v_2)^{n+1}_{j_2-1}}{h_2^2} = (\widetilde{q}_2)^{n+1}_{j_2} + (\widetilde{f}_2)^{n+1}_{j_2} \tag{23}$$

The interface conditions (17) and (18) are discretized as follows:

$$p_1 \frac{(v_1)^{n+1}_{N_1+1} - (v_1)^{n+1}_{N_1}}{h_1} + \alpha_1 (v_1)^{n+1}_{N_1} = \beta_1 (v_2)^n_0 + \widetilde{\gamma}_1^{n+1} \tag{24}$$

$$-p_2 \frac{(v_2)^{n+1}_{0} - (v_2)^{n+1}_{-1}}{h_2} + \alpha_2 (v_2)^{n+1}_{0} = \beta_2 (v_1)^{n+1}_{N_1} + \widetilde{\gamma}_2^{n+1} \tag{25}$$

From (24), we express $(v_1)^{n+1}_{N_1+1}$ and substitute (22) for $j_1 = N_1$ to obtain

$$\begin{aligned}
\frac{(v_1)^{n+1}_{N_1} - (v_1)^n_{N_1}}{\tau} + p_1 \frac{(v_1)^n_{N_1} - (v_1)^n_{N_1-1}}{h_1} + \frac{\alpha_1}{h_1} (v_1)^{n+1}_{N_1} \\
= \frac{\beta_1}{h_2} (v_2)^n_0 + \frac{\gamma_1^{n+1}}{h_1} + (\widetilde{q}_2)^{n+1}_{N_1} + (\widetilde{f}_1)^{n+1}_{N_1}
\end{aligned} \tag{26}$$

Similarly, the substitution of $(v_2)^{n+1}_{-1}$ from (24) to (23) for $j_2 = 0$ yields

$$\begin{aligned}
\frac{(v_2)^{n+1}_{0,s} - (v_2)^n_{0,s}}{\tau} - p_2 \frac{(v_2)^n_{1,s} - (v_2)^n_{0,s}}{h_2} + \frac{\alpha_2}{h_2} (v_2)^{n+1}_{0,s} \\
= \frac{\beta_2}{h_2} (v_1)^{n+1}_{N_1,s} + \frac{\gamma_2^{n+1}}{h_2} + (\widetilde{q}_2)^{n+1}_{0} + (\widetilde{f}_2)^{n+1}_{0}
\end{aligned} \tag{27}$$

The discretizations (22), (23), (26), and (27) are realized in an explicit manner. Let $k_i = p_i \tau / h_i^2$, $\kappa_i = \tau / h_i$, and $i = 1,2$. Thus, we have

$$
\begin{aligned}
(v_1)_{N_1}^{n+1} &= \frac{1}{1+\alpha_1\kappa_1}\Big[(1-p_1\kappa_1)(v_1)_{N_1}^n + p_1\kappa_1(v_1)_{N_1-1}^n + \beta_1\kappa_2(v_2)_0^n \\
&\qquad + \kappa_1\gamma_1^{n+1} + \tau(\widetilde{q}_2)_{N_1}^{n+1} + \tau(\widetilde{f}_1)_{N_1}^{n+1}\Big] \\
(v_1)_{j_1}^{n+1} &= \frac{1}{1+k_1}\Big[(1-k_1)(v_1)_{j_1}^n + k_1(v_{j_1+1}^{n+1} + v_{j_1-1}^n) + \tau(\widetilde{q}_1)_{j_1}^{n+1} + \tau(\widetilde{f}_1)_{j_1}^{n+1}\Big], \\
&\qquad j_1 = N_1-1, N_1-2, \dots, 1 \\
(v_2)_0^{n+1} &= \frac{1}{1+\alpha_2\kappa_2}\Big[(1-p_2\kappa_2)(v_1)_0^n + p_2\kappa_2(v_2)_1^n + \beta_2\kappa_2(v_1)_{N_1}^n \\
&\qquad + \kappa_2\gamma_2^{n+1} + \tau(\widetilde{q}_2)_0^{n+1} + \tau(\widetilde{f}_2)_0^{n+1}\Big] \\
(v_2)_{j_2}^{n+1} &= \frac{1}{1+k_2}\Big[(1-k_2)(v_2)_{j_2}^n + k_2(v_{j_2+1}^n + v_{j_2-1}^{n+1}) + \tau(\widetilde{q}_2)_{j_2}^{n+1} + \tau(\widetilde{f}_2)_{j_2}^{n+1}\Big], \\
&\qquad j_2 = 1, 2, \dots, N_2-1
\end{aligned}
\tag{28}
$$

To obtain the approximate values of $v_1(a_1,t)$ and $v_2(b_2,t)$, as in [41], we use the trapezoidal rule approximation for (19):

$$
\begin{aligned}
(v_1)_0^{n+1} &= \frac{2}{h_1}m_1^{n+1} - \left(2\sum_{j_1=1}^{N_1-1}(v_1)_{j_1}^{n+1} + (v_1)_{N_1}^{n+1}\right) \\
(v_2)_{N_2}^{n+1} &= \frac{2}{h_2}m_2^{n+1} - \left((v_1)_0^{n+1} + 2\sum_{j_1=1}^{N_2-1}(v_1)_{j_1}^{n+1}\right)
\end{aligned}
\tag{29}
$$

Finally, from (20), we obtain

$$
\varphi_1^{n+1} = \frac{(v_1)_0^{n+1}}{\int_c^d \mu_1(y)dy}, \quad \varphi_2^{n+1} = \frac{(v_2)_{N_2}^{n+1}}{\int_c^d \mu_2(y)dy}, \quad n = 1,2,\dots,M \tag{30}
$$

4.2. Numerical Solution of the Direct Problem

In this section, we construct a Saul'yev scheme for solving the direct problem (1)–(9) for an already determined external Dirichlet boundary condition. Let us define the operators

$$
\begin{aligned}
\triangle^-(u_i)_{j_i,s}^{n+1} &= p_i\delta_x(u_i)_{j_i,s}^{(n+1,n)} + q_i\delta_y(u_i)_{j_i,s}^{(n+1,n)} \\
\triangle^+(u_i)_{j_i,s}^{n+1} &= p_i\delta_x(u_i)_{j_i,s}^{(n,n+1)} + q_i\delta_y(u_i)_{j_i,s}^{(n,n+1)}
\end{aligned}
$$

$$
\begin{aligned}
\delta_x(u_i)_{j_i,s}^{(\nu_1,\nu_2)} &= \frac{(u_i)_{j_i+1,s}^{\nu_2} - (u_i)_{j_i,s}^{\nu_2} - (u_i)_{j_i,s}^{\nu_1} + (u_i)_{j_i-1,s}^{\nu_1}}{h_i^2} \\
\delta_y(u_i)_{j_i,s}^{(\nu_1,\nu_2)} &= \frac{(u_i)_{j_i,s+1}^{\nu_2} - (u_i)_{j_i,s}^{\nu_2} - (u_i)_{j_i,s}^{\nu_1} + (u_i)_{j_i,s-1}^{\nu_1}}{h_i^2}
\end{aligned}
$$

The finite difference scheme for (1) and (2) is

$$
\frac{(u_1)_{j_1,s}^{n+1} - (u_1)_{j_1,s}^n}{\tau} - \triangle^+(u_1)_{j_1,s}^{n+1} = (f_1)_{j_1,s}^{n+1},\ j_1 = N_1-1,\dots,1,\ s = N_y-1,\dots,1 \tag{31}
$$

$$
\frac{(u_2)_{j_2,s}^{n+1} - (u_2)_{j_2,s}^n}{\tau} - \triangle^-(u_2)_{j_2,s}^{n+1} = (f_2)_{j_2,s}^{n+1},\ j_2 = 1,\dots,N_2-1,\ s = 1,\dots,N_y-1 \tag{32}
$$

First, we consider the boundary of the discrete domain $\Omega_1^h = \overline{\omega}_{h_1} \times \overline{\omega}_{h_y}$. For the approximation of (5) at the Neumann boundary $y = d$, $a_1 < x_1 < b_1$, we have

$$\frac{(u_1)^{n+1}_{j_1,N_y+1} - (u_1)^{n+1}_{j_1,N_y} + (u_1)^{n}_{j_1,N_y} - (u_1)^{n}_{j_1,N_y-1}}{2h_y} = (g_{1d})^{n+1}_{j_1} \tag{33}$$

Then, from (33), we express $\left((u_1)^{n+1}_{j_1,N_y+1} - (u_1)^{n+1}_{j_1,N_y}\right)/h_y$ and substitute (31) for $s = N_y$ to derive

$$\begin{aligned}\frac{(u_1)^{n+1}_{j_1,N_y} - (u_1)^{n}_{j_1,N_y}}{\tau} = p_1\delta_x(u_1)^{(n,n+1)}_{j_1,N_y} - \frac{2q_1}{h_y}\left(\frac{(u_1)^{n}_{j_1,N_y} - (u_1)^{n}_{j_1,N_y-1}}{h_y} - (g_{1d})^{n+1}_{j_1}\right)\\ +(f_1)^{n+1}_{j_1,N_y},\ \ j_1 = N_1-1,\dots,2,1\end{aligned} \tag{34}$$

At the Neumann boundary $y = c$, $a_1 < x_1 < b_1$, we proceed similarly. We introduce the following approximation of (5):

$$\frac{(u_1)^{n+1}_{j_1,1} - (u_1)^{n+1}_{j_1,0} + (u_1)^{n}_{j_1,0} - (u_1)^{n}_{j_1,-1}}{2h_y} = (g_{1c})^{n+1}_{j_1} \tag{35}$$

By using $(u_1)^{n}_{j_1,0} - (u_1)^{n}_{j_1,-1}$ from (35) and substituting (31) and $s = 0$, we obtain

$$\begin{aligned}\frac{(u_1)^{n+1}_{j_1,0} - (u_1)^{n}_{j_1,0}}{\tau} = p_1\delta^1_x(u_i)^{(n,n+1)}_{j_i,0} + \frac{2q_1}{h_y}\left(\frac{(u_1)^{n+1}_{j_1,1} - (u_1)^{n+1}_{j_1,0}}{h_y} - (g_{1c})^{n+1}_{j_1}\right)\\ +(f_1)^{n+1}_{j_1,0},\ \ j_1 = N_1-1,\dots,2,1\end{aligned} \tag{36}$$

At the interface boundary $x_1 = b_1$, $c < y < d$, we construct the following approximation of (7):

$$\frac{(u_1)^{n+1}_{N_1+1,s} - (u_1)^{n+1}_{N_1,s} + (u_1)^{n}_{N_1,s} - (u_1)^{n}_{N_1-1,s}}{2h_1} + \alpha_1(u_1)^{n+1}_{N_1+1,s} = \beta_1(u_2)^{n}_{0,s} + (\gamma_1)^{n+1}_{s} \tag{37}$$

By using $((u_1)^{n+1}_{N_1+1,s} - (u_1)^{n+1}_{N_1,s})/h_1$ from (37) and applying (31) for $j_1 = N_1$, we obtain

$$\begin{aligned}\frac{(u_1)^{n+1}_{N_1,s} - (u_1)^{n}_{N_1,s}}{\tau} + \frac{2\alpha_1}{h_1}(u_1)^{n+1}_{N_1,s} = q_1\delta_y(u_1)^{(n,n+1)}_{N_1,s} - \frac{2p_1}{h_1^2}\left((u_1)^{n}_{N_1,s} - (u_1)^{n}_{N_1-1,s}\right)\\ +\frac{2\beta_1}{h_1}(u_2)^{n}_{0,s} + \frac{2(\gamma_1)^{n+1}_{s}}{h_1} + (f_1)^{n+1}_{N_1,s},\ \ j_1 = N_1-1,\dots,2,1\end{aligned} \tag{38}$$

We consider corner nodes ($x_1 = a_1, y = c$) and ($x_1 = a_1, y = d$), where the interface boundary intersects Neumann boundaries. Using (33), $j_1 = N_1$, (37), $s = N_y$, (35), $j_1 = 0$, (37), and $s = 0$, we derive

$$\begin{aligned}\frac{(u_1)^{n+1}_{N_1,0} - (u_1)^{n}_{N_1,0}}{\tau} + \frac{2\alpha_1}{h_1}(u_1)^{n+1}_{N_1,0} + \frac{2q_1}{h_y^2}((u_1)^{n+1}_{N_1,0} - (u_1)^{n+1}_{N_1,1}) = -\frac{2q_1}{h_1}(g_{1c})^{n}_{N_1}\\ -\frac{2p_1}{h_1^2}\left((u_1)^{n}_{N_1,0} - (u_1)^{n}_{N_1-1,0}\right) + \frac{2\beta_1}{h_1}(u_2)^{n}_{0,s} + \frac{2(\gamma_1)^{n+1}_{0}}{h_1} + (f_1)^{n+1}_{N_1,0}\end{aligned} \tag{39}$$

$$\frac{(u_1)_{N_1,N_y}^{n+1}-(u_1)_{N_1,N_y}^{n}}{\tau}+\frac{2\alpha_1}{h_1}(u_1)_{N_1,N_y}^{n+1}=\frac{2q_1}{h_y}\left((g_{1d})_{N_1}^{n+1}-\frac{(u_1)_{N_1,N_y}^{n}-(u_1)_{N_1,N_y-1}^{n}}{h_y}\right)$$
$$-\frac{2p_1}{h_1^2}\left((u_1)_{N_1,N_y}^{n}-(u_1)_{N_1-1,N_y}^{n}\right)+\frac{2\beta_1}{h_1}(u_2)_{0,N_y}^{n}+\frac{2(\gamma_1)_0^{n+1}}{h_1}+(f_1)_{N_1,N_y}^{n+1} \tag{40}$$

The discrete Dirichlet boundary condition at $x=a_1$, $c\le y\le d$ is the standard

$$(u_1)_{0,s}^{n+1}=\varphi_1^{n+1}(\mu_1)_s,\quad s=N_y,N_y-1,\dots,1 \tag{41}$$

Therefore, the second kind Saul'yev finite difference scheme in the domain $\overline{\omega}_{h_1}\times\overline{\omega}_{h_y}\times\overline{\omega}_\tau$ is formed by Equations (31), (34), (36), and (38)–(41) and initial condition $(u_1)_{j_1,s}^{0}=u_1^0(x_{1j_1},y_s)$. Note that at each time layer, this discretization is independent of the solution in the second domain and can be executed in an explicit fashion as well.

Further, we construct the corresponding discretizations at the boundary of the second domain: $\Omega_2^h=\overline{\omega}_{h_2}\times\overline{\omega}_{h_y}$. At each time level, we compute the solution first in Ω_1^h and then in Ω_2^h, so that the solution u_1^{n+1} is already known. We proceed in the same manner as for the construction of the numerical scheme in Ω_1^h but take into account that now, we move from the bottom left corner to the upper right corner, and first kind Saul'yev formula is used. The resulting discretizations for (4), (6), and (8) at the boundary grid nodes are as follows:

$$\frac{(u_2)_{0,0}^{n+1}-(u_2)_{0,0}^{n}}{\tau}+\frac{2\alpha_2}{h_2}(u_2)_{0,0}^{n+1}=\frac{2p_2}{h_2^2}\left((u_2)_{1,0}^{n}-(u_2)_{0,0}^{n}\right)+\frac{2q_2}{h_y^2}\left((u_2)_{0,1}^{n}-(u_2)_{0,0}^{n}\right)$$
$$+\frac{2\beta_2}{h_2}(u_1)_{N_1,0}^{n+1}+\frac{2(\gamma_2)_0^{n+1}}{h_2}-\frac{2q_2}{h_y}(g_{2c})_0^{n+1}+(f_2)_{0,0}^{n+1} \tag{42}$$

$$\frac{(u_2)_{j_2,0}^{n+1}-(u_2)_{j_2,0}^{n}}{\tau}=p_2\delta_x(u_2)_{j_2,0}^{(n+1,n)}$$
$$+\frac{2q_2}{h_y^2}\left((u_2)_{j_2,1}^{n+1}-(u_2)_{j_2,0}^{n+1}\right)-\frac{2q_2}{h_y}(g_{2c})_{j_2}^{n+1},\quad j_2=1,2,\dots,N_2-1 \tag{43}$$

$$\frac{(u_2)_{0,s}^{n+1}-(u_2)_{0,s}^{n}}{\tau}+\frac{2\alpha_2}{h_2}(u_2)_{0,s}^{n+1}=q_2\delta_y(u_2)_{0,s}^{(n+1,n)}-\frac{2p_2}{h_2^2}\left((u_2)_{0,s}^{n}-(u_2)_{1,s}^{n}\right)$$
$$+\frac{2\beta_2}{h_2}(u_1)_{N_1,s}^{n+1}+\frac{2(\gamma_2)_s^{n+1}}{h_2}+(f_2)_{0,s}^{n+1},\quad s=1,2,\dots,N_y-1 \tag{44}$$

$$\frac{(u_2)_{0,N_y}^{n+1}-(u_2)_{0,N_y}^{n}}{\tau}+\frac{2\alpha_2}{h_2}(u_2)_{0,N_y}^{n+1}+\frac{2q_2}{h_y^2}\left((u_2)_{0,N_y}^{n+1}-(u_2)_{0,N_y-1}^{n+1}\right)+\frac{2\beta_2}{h_2}(u_1)_{N_1,N_y}^{n+1}$$
$$=\frac{2p_2}{h_2^2}\left((u_2)_{1,N_y}^{n}-(u_2)_{0,N_y}^{n}\right)+\frac{2(\gamma_2)_{N_y}^{n+1}}{h_2}+\frac{2q_2}{h_y}(g_{2c})_{N_y}^{n+1}+(f_2)_{0,N_y}^{n+1} \tag{45}$$

$$\frac{(u_2)_{j_2,N_y}^{n+1}-(u_2)_{j_2,N_y}^{n}}{\tau}+\frac{2q_2}{h_y^2}\left((u_2)_{j_2,N_y}^{n+1}-(u_2)_{j_2,N_y-1}^{n+1}\right)$$
$$=p_2\delta_x(u_2)_{j_2,N_y}^{(n+1,n)}+\frac{2q_2}{h_y}(g_{2d})_{j_2}^{n+1},\quad j_1=1,2,\dots,N_2-1 \tag{46}$$

$$(u_2)_{N_2,s}^{n+1}=\varphi_2^{n+1}(\mu_2)_s,\quad s=1,2,\dots,N_y \tag{47}$$

The finite difference scheme in the second domain Ω_2^h is formed by Equations (32) and (42)–(47) and initial condition $(u_1)^0_{j_1,s} = u_1^0(x_{1j_1}, y_s)$.

5. Numerical Tests

In this section, we illustrate the efficiency of the developed numerical method for solving the IP. The test example is (1)–(9) with the following parameters:

$$a_1 = 1,\ b_1 = 2,\ a_2 = 3,\ b_2 = 4,\ c = 0,\ d = 1,\ T = 1$$
$$p_1 = 2,\ p_2 = 3,\ q_1 = 2,\ q_2 = 1.5,\ \alpha_1 = 3,\ \alpha_2 = 1,\ \beta_1 = 2,\ \beta_2 = 0.5$$

We deal with exact measurements (48) and the exact solution of the problem (1)–(9) in order to verify the accuracy. The computations are performed for $h = h_1 = h_2 = h_y$ ($N = N_1 = N_2 = N_y$) and $\tau = h^2$. We give errors in the maximal discrete norm (ε_i, $\mathcal{E}_i$) and the order of convergence (cr_i, CR_i) of the recovered functions φ_i^n and solutions $(u_i)^n_{j_i,s}$, obtained for φ_i^n, in comparison with the corresponding exact ones $\varphi(t)$ and $u_i(x, y, t)$, $i = 1, 2$.

$$\varepsilon_i = \varepsilon_i(M) \max_{0\le n\le M} |\varphi_i(t_n) - \varphi_i^n|,\ \ \mathcal{E}_i = \mathcal{E}_i(N) = \max_{0\le n\le M} \max_{0\le j_i\le N} \max_{0\le s\le N} |u_i(x_{j_i}, y_s, t_n) - (u_i)^n_{j_i,s}|,$$
$$cr_i = \log_2 \frac{\varepsilon_i(M)}{\varepsilon_i(2M)},\ \ CR_i = \log_2 \frac{\mathcal{E}_i(N)}{\mathcal{E}_i(2N)}.$$

Example 1 (*Convergence test*)**.** *We take the following functions in the model problem* (1)–(9)*:*

$$f_1(x, y, t) = e^{\lambda_1 t}\left(\frac{\pi^2}{8} + \lambda_1\right)\left(\cos\frac{\pi x}{4} + \cos\frac{\pi y}{4}\right)$$
$$f_2(x, y, t) = e^{\lambda_2 t}\left[\left(\frac{3\pi^2}{8} + \lambda_2\right)\left(\cos\frac{\pi x}{4} + \cos\frac{\pi y}{4}\right) + \frac{3\pi^2}{8}\cos\frac{\pi x}{2}\right]$$
$$\gamma_1(y, t) = e^{\lambda_1 t}\left(3\cos\frac{\pi y}{4} - \frac{\pi}{2}\right) - 2e^{\lambda_2 t}\cos\frac{\pi y}{2}$$
$$\gamma_2(y, t) = e^{\lambda_2 t}\left(\frac{3\pi}{2} + \cos\frac{\pi y}{2}\right) - \frac{1}{2}e^{\lambda_1 t}\cos\frac{\pi y}{4}$$
$$\mu_1(y) = \frac{\sqrt{2}}{2} + \cos\frac{\pi y}{4},\ \ \mu_1(y) = \cos\frac{\pi y}{4} - 1,\ \ \varphi_1(t) = e^{\lambda_1 t},\ \ \varphi_2(t) = e^{\lambda_2 t}$$
$$u_1^0(x, y) = \cos\frac{\pi x}{4} + \cos\frac{\pi y}{4},\ \ u_2^0(x, y) = \cos\frac{\pi x}{2} + \cos\frac{\pi y}{2}$$

Then, the exact solution of (1)–(9) *is*

$$u_1(x, y, t) = e^{\lambda_1 t}\left(\cos\frac{\pi x}{4} + \cos\frac{\pi y}{4}\right),\ \ u_2(x, y, t) = e^{\lambda_2 t}\left(\cos\frac{\pi x}{2} + \cos\frac{\pi y}{2}\right)$$

and in view of (19)*, the exact measured functions are*

$$m_1(t) = \frac{4}{\pi}e^{\lambda_1 t},\ \ m_2(t) = \frac{4}{\pi}e^{\lambda_2 t}. \tag{48}$$

The computational results for $\lambda_1 = -1/2$, $\lambda_2 = -1/3$ and $\lambda_1 = 1$, $\lambda_2 = -2$ are listed in Tables 1 and 2, respectively. We observe that for both tests, the order of convergence of the recovered functions φ_i is first.

In Tables 3 and 4, we give the errors of the corresponding numerical solutions, computed for recovered functions φ_i with both sets of parameters λ_i, $i = 1, 2$. The results show that the numerical method is convergent of order one.

In Figure 2, we plot the error (i.e., $u_i(x_{j_i}, y_s, t_n) - (u_i)^n_{j_i,s}$) of the numerical solution of the 2D direct problem at the final time for $\lambda_1 = -1/2$, $\lambda_2 = -1/3$ and $\lambda_1 = 1$, $\lambda_2 = -2$.

Table 1. Errors and convergence rate of φ_1^n and φ_2^n, $\lambda_1 = -1/2$, $\lambda_2 = -1/3$, Example 1.

N	ε_1	cr_1	ε_2	cr_2
20	3.6480×10^{-3}		5.7428×10^{-3}	
40	1.7277×10^{-3}	1.0782	3.2817×10^{-3}	0.8073
80	8.4978×10^{-4}	1.0237	1.8136×10^{-3}	0.8556
160	4.2181×10^{-4}	1.0105	9.5262×10^{-4}	0.9289
320	2.1017×10^{-4}	1.0050	4.8802×10^{-4}	0.9650
640	1.0491×10^{-4}	1.0025	2.4697×10^{-4}	0.9826

Table 2. Errors and convergence rate of φ_1^n and φ_2^n, $\lambda_1 = 1$, $\lambda_2 = -2$, Example 1.

N	ε_1	cr_1	ε_2	cr_2
20	1.5829×10^{-2}		2.2918×10^{-2}	
40	7.8168×10^{-3}	1.0179	1.0155×10^{-2}	1.1743
80	3.8849×10^{-3}	1.0087	4.9144×10^{-3}	1.0471
160	1.9367×10^{-3}	1.0043	2.4263×10^{-3}	1.0183
320	9.6692×10^{-4}	1.0021	1.2062×10^{-3}	1.0083
640	4.8310×10^{-4}	1.0011	6.0141×10^{-4}	1.0040

Table 3. Errors and convergence rate of $(u_1)^n$ and $(u_2)^n$, $\lambda_1 = -1/2$, $\lambda_2 = -1/3$, Example 1.

N	$\mathcal{E}_1$	CR_1	$\mathcal{E}_2$	CR_2
20	6.2275×10^{-3}		1.1486×10^{-2}	
40	2.9494×10^{-3}	1.0782	6.5635×10^{-3}	0.8073
80	1.4507×10^{-3}	1.0237	3.6273×10^{-3}	0.8556
160	7.2008×10^{-4}	1.0105	1.9052×10^{-3}	0.9289
320	3.5879×10^{-4}	1.0050	9.7604×10^{-4}	0.9650
640	1.7907×10^{-4}	1.0026	4.9230×10^{-4}	0.9874

Table 4. Errors and convergence rate of $(u_1)^n$ and $(u_2)^n$, $\lambda_1 = 1$, $\lambda_2 = -2$, Example 1.

N	$\mathcal{E}_1$	CR_1	$\mathcal{E}_2$	CR_2
20	2.7022×10^{-2}		4.5835×10^{-2}	
40	1.3344×10^{-2}	1.0179	2.0309×10^{-2}	1.1743
80	6.6320×10^{-3}	1.0087	9.8288×10^{-3}	1.0471
160	3.3061×10^{-3}	1.0043	4.8525×10^{-3}	1.0183
320	1.6506×10^{-3}	1.0021	2.4123×10^{-3}	1.0083
640	8.2469×10^{-4}	1.0011	1.2032×10^{-3}	1.0035

Example 2 (*Noisy data*)**.** *We repeat the same experiment as in Example 1, but now, we give a noise to the measurements:*

$$m_i^{\sigma_i}(t_n) = m_i(t_n) + 2\sigma_i m_i(t_n)(\rho_i(t_n) - 0.5), \quad i = 1, 2$$

where σ_i is the noise level and $\rho_i(t_n)$ is a random function, uniformly distributed on the interval $[0, 1]$. *Then, we smooth the data through polynomial curve-fitting of the third degree.*

In Figures 3 and 4 we present exact and recovered functions φ_i, $i = 1, 2$ for $N = 80$, $\sigma_1 = 0.02$, $\sigma_1 = 0.03$, with parameters $\lambda_1 = -1/2$, $\lambda_2 = -1/3$ and $\lambda_1 = 1$, $\lambda_2 = -2$, respectively. The algorithm successfully restores the external boundary conditions. The largest error is close to the initial time.

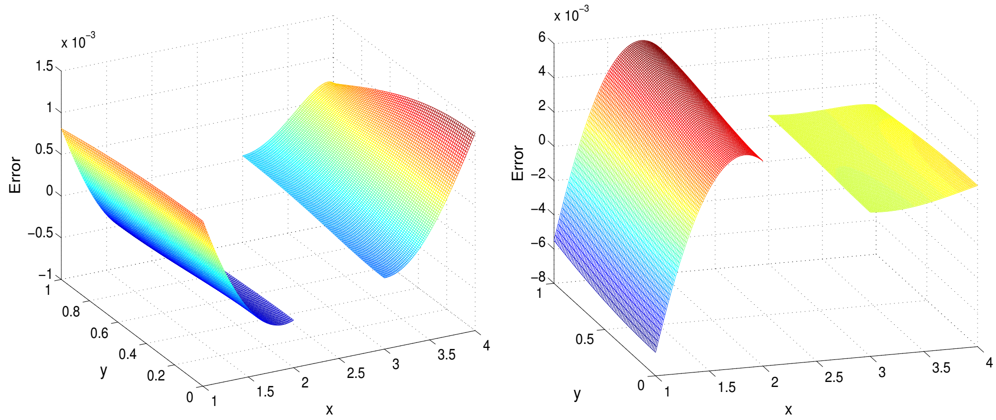

Figure 2. Error of the numerical solution, $\lambda_1 = -1/2$, $\lambda_2 = -1/3$ (**left**) and $\lambda_1 = 1$, $\lambda_2 = -2$ (**right**), $N = 80$, Example 1.

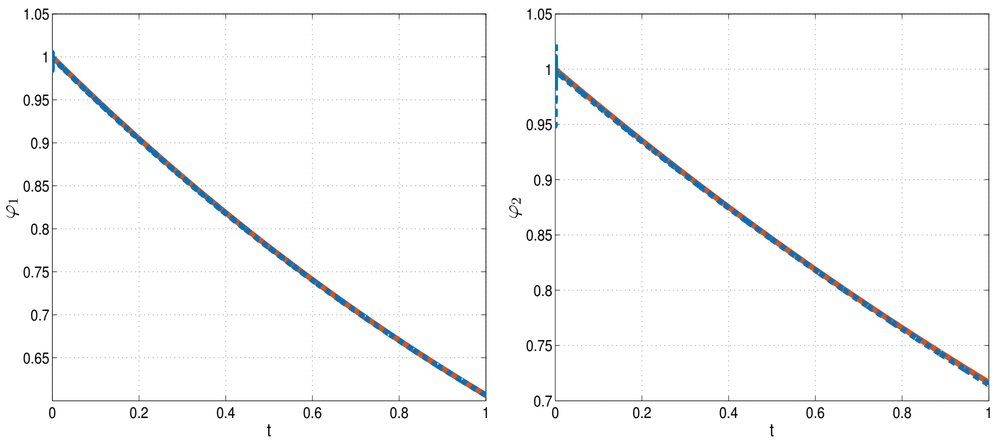

Figure 3. Exact and recovered functions φ_1 (**left**) and φ_2 (**right**), $N = 80$, $\sigma_1 = 0.02$, $\sigma_1 = 0.03$, $\lambda_1 = -1/2$, $\lambda_2 = -1/3$, Example 2.

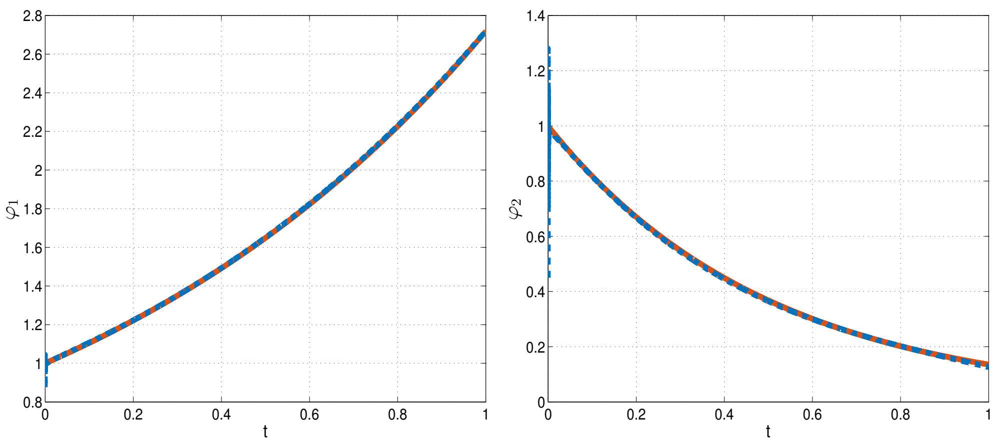

Figure 4. Exact and recovered functions φ_1 (**left**) and φ_2 (**right**), $N = 80$, $\sigma_1 = 0.02$, $\sigma_1 = 0.03$, $\lambda_1 = 1$, $\lambda_2 = -2$, Example 2.

The corresponding errors of the recovered solution u_i at the final time layer are depicted in Figure 5. The precision is quite satisfactory. Therefore, we may conclude that the method is efficient also for noisy measurements.

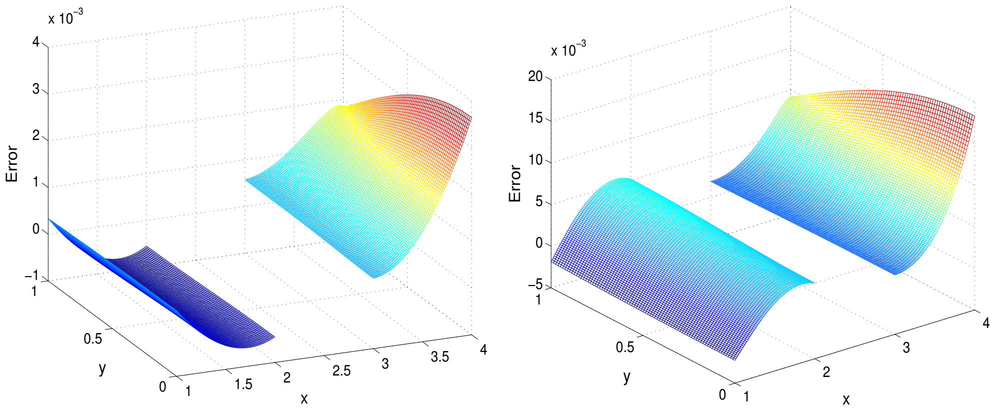

Figure 5. Error of the recovered solutions u_1 and u_2, $N = 80$, $\sigma_1 = 0.02$, $\sigma_1 = 0.03$ and $\lambda_1 = -1/2$, $\lambda_2 = -1/3$ (**left**), $\lambda_1 = 1$, $\lambda_2 = -2$ (**right**), Example 2.

6. Conclusions

This paper concerns an initial boundary-value problem for a two-dimensional heat equation, defined on disjoint domains. It is a special interface parabolic problem, in which the interface boundary conditions are of Robin's type, while the external boundary conditions are of Dirichlet and Neumann form. We first establish the well-posedness of the direct (forward) problem. The Dirichlet conditions are unknown functions for the inverse problem and have to be determined on the basis of two integral observations—one on each rectangle. We reduce the inverse problem to a direct one with Dirichlet boundary conditions and integral conditions on the interface of the corresponding rectangle. We prove the well-posedness of the new problem, and as a consequence, the well-posedness of the original inverse problem follows.

The new, non-local problem is solved using the Saul'yev explicit difference scheme. Computational tests showed that the order of convergence of the numerical method for exact data is first. For noisy measurements, we show that the algorithm successfully restores external boundary conditions, and the precision of the solution is optimal.

The main advantage of the proposed method is that the 2D ill-posed problem is reduced to a 1D well-posed problem. Moreover, the numerical discretization is unconditionally stable and can be realized explicitly. The disadvantages are that the method is first-order accurate (for exact measurements) and conditionally consistent.

An even more challenging problem is to reconstruct the reaction space-dependent coefficient using integral observations. We hope to be able to address these issues and to report additional progress in the future.

Author Contributions: Conceptualization, M.N.K. and L.G.V.; methodology, M.N.K. and L.G.V.; investigation, M.N.K. and L.G.V.; resources, M.N.K. and L.G.V.; writing—original draft preparation, M.N.K. and L.G.V.; writing—review and editing, L.G.V.; validation, M.N.K. All authors have read and agreed to the published version of the manuscript.

Funding: This study is financed by the European Union–NextGenerationEU, through the National Recovery and Resilience Plan of the Republic of Bulgaria, project no. BG-RRP-2.013-0001-C01.

Data Availability Statement: Data are contained within the article.

Acknowledgments: The authors are very grateful to the anonymous reviewers, whose valuable comments and suggestions improved the quality of this paper.

Conflicts of Interest: The authors declare no conflicts of interest.

Abbreviations

The following abbreviations and nomenclature are used in this manuscript:

$\Omega_i, i = 1,2$	Spatial disconnected domains
p_i	Diffusion coefficient in ith domain
q_i	Diffusion coefficient in ith domain
f_i	Heat source function in ith domain
α_i, β_i	Reaction coefficients in interface conditions in ith domain
$\mu_i(y)$	Space-dependent part of the external boundary conditions in ith domain
$\varphi_i(t)$	Time-dependent part of the external boundary conditions in ith domain
$\gamma_i(y,t)$	Interface boundary source in ith domain
$g_{ic}(x,t)$	Dirichlet boundary source at $y = c$ in ith domain
$g_{id}(x,t)$	Dirichlet boundary source at $y = d$ in ith domain
IP	Inverse problem

References

1. Lesnic, D. *Inverse Problems with Applications in Science and Engineering*; CRC Press: Abingdon, UK, 2021; p. 349.
2. Samarskii, A.A.; Vabishchevich, P.N. *Numerical Methods for Solving Inverse Problems in Mathematical Physics*; de Gruyter: Berlin, Germany, 2007; 438p.
3. Hasanov, A.H.; Romanov, V.G. *Introduction to Inverse Problems for Differential Equations*, 1st ed.; Springer: Cham, Switzerland, 2017; 261p.
4. Isakov, V. *Inverse Problems for Partial Differential Equations*, 3rd ed.; Springer: Cham, Switzerland, 2017; p. 406.
5. Ivanov, V.K.; Vasin, V.V.; Tanana, V.P. *Theory of Linear Ill-Posed Problems and Its Approximations*; Nauka: Moscow, Russia, 1978. (In Russian)
6. Kabanikhin S.I. *Inverse and Ill-Posed Problems*; DeGruyer: Berlin, Germany, 2011.
7. Prilepko, A.I.; Orlovsky, D.G.; Vasin, I.A. *Methods for Solving Inverse Problems in Mathematical Physics*; Marcel Dekker: New York, NY, USA, 2000.
8. Rundell, W.; Yin, H.-M. A parabolic inverse problem with an unknown boundary condition. *J. Differ. Equ.* **1990**, *86*, 234–242. [CrossRef]
9. Demir, A.; Ozbilge, E. Identification of the unknown boundary condition in a linear parabolic equation. *J. Inequal. Appl.* **2013**, *96*, 1–7. [CrossRef]
10. Vasil'ev, V.I.; Su, L. Numerical method for solving boundary inverse problem for one-dimensional parabolic equation. *Math. Model.* **2017**, *24*, 108–117. [CrossRef]
11. Rundell, W.; Xub, X.; Zuo, L. The determination of an unknown boundary condition in a fractional diffusion equation. *Appl. Anal.* **2013**, *92*, 1511–1526. [CrossRef]
12. Zheng, G.H.; Wei, T. A new regularization method for a Cauchy problem of the time fractional diffusion equation. *Adv. Comput. Math.* **2012**, *36*, 377–398. [CrossRef]
13. Abdollahi, A.N.; Rostamy, D. Identifying an unknown time-dependent boundary source in time-fractional diffusion equation with a non-local boundary condition. *J. Comput. Appl. Math.* **2019**, *355*, 3–50.
14. Zheng, G.H.; Wei, T. Spectral regularization method for a Cauchy problem of the time fractional advection-dispersion equation *J. Comput. Appl. Math.* **2010**, *233*, 2631–2640. [CrossRef]
15. Kumar, S.; Ghosh, S.; Samet, B.; Goufo, E.F.D. An analysis for heat equations arises in diffusion process using new Yang-Abdel-Aty-Cattani fractional operator. *Math. Method Appl. Sci.* **2020**, *43*, 6062–6080. [CrossRef]
16. Rasheed, M.; Ali, A.H.; Alabdali, O.; Shihab, S.; Rashid, A.; Rashid, T.; Hamad, S.H.A. The effectiveness of the finite differences method on physical and medical images based on a heat diffusion equation. *J. Phys. Conf. Ser.* **2021**, *1999*, 012080. [CrossRef]
17. Liu, C.; Ball, W.P. Analytical modeling of diffusion-limited contamination and decontamination in a two-layer porous medium. *Adv. Water Resour.* **1998**, *21*, 297–313. [CrossRef]
18. Sheils, N.E. Multilayer diffusion in a composite medium with imperfect contact. *Appl. Math. Model.* **2017**, *46*, 450–464. [CrossRef]
19. Raza, A.; Stadoleanu, O.V.; Abed, A.M.; Ali, A.H.; Sallah, M. Heat transfer model analysis of fractional Jeffery-type hybrid nanofluid dripping through a poured microchannel. *Int. J. Thermofluids* **2024**, *22*, 100656. [CrossRef]
20. Amir, M.; Ali, Q.; Raza, A.; Almusawa, M.Y.; Hamali, W.; Ali, A.H. Computational results of convective heat transfer for fractionalized Brinkman type tri-hybrid nanofluid with ramped temperature and non-local kernel. *Ain Shams Eng. J.* **2024**, *15*, 102576. [CrossRef]
21. Carr, E.J. Generalized semi-analytical solution for coupled multispecies advection-dispersion equations in multilayer porous media. *Appl. Math. Model.* **2021**, *94*, 87–97. [CrossRef]
22. Carr, E.J. New semi-analytical solutions for advection–dispersion equations in multilayer porous media. *Transp. Porous Med.* **2020**, *135*, 39–58. [CrossRef]
23. Chen, J.-S.; Ho, Y.-C.; Liang, C.-P.; Wang, S.-W.; Liu, C.-W. Semi-analytical model for coupled multispecies advective-dispersive transport subject to rate-limited sorption. *J. Hydrol.* **2019**, *579*, 124164. [CrossRef]

24. March, N.G.; Carr, E.J. Finite volume schemes for multilayer diffusion. *J. Comput. Appl. Math.* **2019**, *345*, 206–223. [CrossRef]
25. Amosov, A.A. Global solvability of a nonlinear nonstationary problem with a nonlocal boundary condition of radiation heat transfer type. *Differ. Equ.* **2005**, *41*, 96–109. [CrossRef]
26. Jovanovic, B.S.; Vulkov, L.G. Finite difference approximation of strong solutions of a parabolic interface problem on disconected domains. *Publ. Inst. Math.* **2008**, *84*, 37–48 [CrossRef]
27. Jovanovic, B.S.; Vulkov, L.G. Numerical solution of a two-dimensional parabolic transmission problem. *Int. J. Numer. Anal. Model.* **2010**, *7*, 156–172.
28. Koleva, M.N.; Vulkov, L.G. Weak and classical solutions to multispecies advection-dispersion equations in multilayer porous media. *Mathematics* **2023**, *11*, 3103. [CrossRef]
29. Milovanović, Z. Finite Difference Scheme for a Parabolic Transmission Problem in Disjoint Domains. In *Numerical Analysis and Its Applications, Lecture Notes in Computer Science*; Dimov, I., Faragó, I., Vulkov, L., Eds.; Springer: Berlin/Heidelberg, Germany, 2013; Volume 8236, pp. 403–410.
30. Mikhailov, M.D.; Oezisik, M.N.; Vulchanov, N.L. Diffusion in composite layers with automatic solution of the eigenvalue problem. *Int. J. Heat Mass Transfer* **1983**, *26*, 1131–1141. [CrossRef]
31. Asvestas, M.; Sifalakis, A.G.; Papadopoulou, E.P.; Saridakis, Y.G. Fokas method for a multi-domain linear reaction-diffusion equation with discontinuous diffusivity. *J. Phys. Conf. Ser.* **2014**, *490*, 012143. [CrossRef]
32. Movahedian, B.; Boroomand, B. The solution of direct and inverse transient heat conduction problems with layered materials using exponential basis functions. *Int. J. Therm. Sci.* **2014**, *77*, 186–198. [CrossRef]
33. Koleva, M.N.; Vulkov, L.G. Numerical identification of external boundary conditions for time fractional parabolic equations on disjoint domains. *Fractal Fract.* **2023**, *7*, 326. [CrossRef]
34. Koleva, M.N.; Vulkov, L.G. *Reconstruction of Boundary Conditions of a Parabolic-Hyperbolic Transmission Problem*; Springer Series Proc. in Mathematics & Statistics, to Appear; Springer: Berlin/Heidelberg, Germany, 2024.
35. Saul'yev, V.K. *Integration of Equation Parabolic Type by the Method of Nets*; Pergamon Press: New York, NY, USA, 1964.
36. Bieniasz, L.K.; Østerby, O.; Britz, D. Numerical stability of the Saul'yev finite difference algorithms for electrochemical kinetic simulations: Matrix stability analysis for an example problem involving mixed boundary conditions. *Comput. Chem.* **1995**, *19*, 357–370. [CrossRef]
37. Pourghanbar, S.; Manafian, J.; Ranjbar, M.; Aliyeva, A.; Gasimov, Y.S. An efficient alternating direction explicit method for solving a nonlinear partial differential equation. *Math. Probl. Eng.* **2020**, *2020*, 9647416. [CrossRef]
38. Vongkok, A.; Pochai, N. Numerical simulations for reactive nitrogen compounds pollution measurements in a stream using Saulyev method. *Ital. J. Pure Appl. Math.* **2020**, *43*, 552–582.
39. Yang, J.; Li, Y.; Lee, C.; Lee, H.G.; Kwok, S.; Hwang, Y.; Xin, X.; Kim, J. An explicit conservative Sayl'yev scheme for the Cahn-Hillard equation, Intern. *J. Mech. Sci.* **2022**, *217*, 106985. [CrossRef]
40. Zhu, L. A Second-order uniformly stable explicit asymmetric discretization method for one-dimensional fractional diffusion equations. *Complexity* **2019**, *2019*, 4238420. [CrossRef]
41. Dehghang, M. Saul'yev techniques for solving a parabolic equations with a nonlinear boundary specification, Intern. *J. Comput. Math.* **2003**, *80*, 257–265.
42. Jovanovic, B.S.; Vulkov, L.G. Formulation and analysis of a parabolic transmission problem on disjoint intervals. *Publ. L'Inst. Math.* **2012**, *91*, 111–123. [CrossRef]
43. Wloka, J. *Partial Differential Equations*; Cambridge University Press: Cambridge, UK, 1987.
44. Ladyzhenskaia, O.A.; Solonnikov, V.A.; Ural'tseva, N.N. *Linear and Quasi-Linear Equations of Parabolic Type*; American Mathematical Society: Ann Arbor, MI, USA, 1968; 648p.
45. Darvishi, T. Forward-Backward Saul'yev Method to Solve PDEs. *WSEAS Trans. Math.* **2003**, *2*, 21–25.